

This discussion paper is/has been under review for the journal Atmospheric Chemistry and Physics (ACP). Please refer to the corresponding final paper in ACP if available.

# Numerical simulation of flow, H<sub>2</sub>SO<sub>4</sub> cycle and new particle formation in the CERN CLOUD chamber

J. Voigtländer<sup>1</sup>, J. Duplissy<sup>2</sup>, and F. Stratmann<sup>1</sup>

<sup>1</sup>Leibniz Institute for Tropospheric Research, Leipzig, Germany

<sup>2</sup>CERN, PH Department, Geneva, Switzerland

Received: 24 June 2011 – Accepted: 6 July 2011 – Published: 14 July 2011

Correspondence to: J. Voigtländer (jensv@tropos.de)

Published by Copernicus Publications on behalf of the European Geosciences Union.

## Numerical simulations of the CLOUD chamber

J. Voigtländer et al.

Title Page

Abstract

Introduction

Conclusions

References

Tables

Figures

⏪

⏩

◀

▶

Back

Close

Full Screen / Esc

Printer-friendly Version

Interactive Discussion



## Abstract

To study the effect of galactic cosmic rays on aerosols and clouds, the Cosmic Leaving Outdoor Droplets (CLOUD) project was established. Experiments are carried out at a 26 m<sup>3</sup> tank at CERN (Switzerland). In the experiments, the effect of ionising particle radiation on H<sub>2</sub>SO<sub>4</sub> particle formation and growth is investigated. To evaluate the experimental configuration, the experiment was simulated using a coupled multi-dimensional CFD – particle model (CLOUD-FPM). In the model the coupled fields of gas/vapour species, temperature, flow velocity and particle properties were computed to investigate the tank's mixing state and mixing times. Simulation results show that the mixing state of the tank's contents largely depends on the characteristics of the mixing fans and a 1-fan configuration, as used in first experiments, may not be sufficient to ensure a homogeneously mixed chamber. To mix the tank properly, 2 fans are necessary. The 1/e response times for instantaneous changes of wall temperature and saturation ratio inside the chamber were found to be in the order of few minutes. Particle nucleation and growth was also simulated and particle number size distribution properties of the freshly nucleated particles (particle number, mean size, standard deviation of the assumed log-normal distribution) were found to be mixed over the tank's volume similar to the gas species.

## 1 Introduction

Atmospheric aerosols are complicated multiphase systems, influencing earth' climate directly via absorption and scattering of solar radiation and indirectly via cloud processes. Key parameters for physical and chemical behaviour are micro-physical properties, i.e., particle/droplet number size distribution and chemical composition of the particles. However, the processes, which control these properties are not well understood. Largest uncertainties in understanding the current climate change are contributed to aerosols and clouds (IPCC2007, 2007). These uncertainties partly result

### Numerical simulations of the CLOUD chamber

J. Voigtländer et al.

Title Page

Abstract

Introduction

Conclusions

References

Tables

Figures



Back

Close

Full Screen / Esc

Printer-friendly Version

Interactive Discussion



from solar-related contributions, such as the effects of galactic cosmic rays on aerosols and clouds (Svensmark and Friis-Christensen, 1997; Carslaw et al., 2002), and requires further research.

To investigate the effect of galactic cosmic rays on particle nucleation, the Cosmic Leaving Outdoor Droplets (CLOUD) project was established. Within this project, experiments are carried out at a large volume cloud chamber ( $26\text{ m}^2$ ), located at CERN (Switzerland). In the CLOUD-09 chamber, aerosol particles, cloud droplets and ice crystals can be exposed to simulated atmospheric conditions and a particle beam provided by the CERN Proton Synchrotron (PS) particle accelerator. The chamber is equipped with a large number of different instruments to study aerosol-cloud-cosmic rays micro-physics under well defined conditions. Results of the pilot experiments were already presented in Duplissy (2010).

A big issue in large volume cloud chambers like the CLOUD-09 chamber at CERN is to achieve spatial homogeneity. This includes thermodynamic conditions, gas composition and particle properties. Homogeneity in the tank becomes more complicated, if several parameters are changed during the experiments (e.g. via UV-illumination system, particle nucleation, trace gas input, wall cooling). To achieve homogeneity, mixing fans are usually applied in such experiments. To check the mixing state, measurements are made at several selected points. However, it is not possible to check all parameters continuously. Therefore, numerical simulations are helpful and necessary.

A theoretical study about cloud droplet formation in a similar (shape, aspect ratio), but smaller ( $12\text{ m}^2$ ) cloud tank was already given by Schütze and Stratmann (2008). It was stated that a 1-fan configuration should be, due to large wall effects, avoided and replaced by 2 fans with a face to face configuration. However, simulations presented in Schütze and Stratmann (2008) were not performed for the actual CLOUD geometry and not evaluated with experimental cloud chamber data.

This paper presents numerical simulation results for a cloud tank with the geometry of the CLOUD-09 chamber in comparison to experimental data. Aim of the study was to evaluate the mixing state with respect to both, gaseous species and particles.

## Numerical simulations of the CLOUD chamber

J. Voigtländer et al.

Title Page

Abstract

Introduction

Conclusions

References

Tables

Figures

◀

▶

◀

▶

Back

Close

Full Screen / Esc

Printer-friendly Version

Interactive Discussion



Simulations were carried out using a coupled computational fluid dynamics (CFD) – particle model (CLOUD-FPM). After a very brief description of the experimental set-up, fundamental aspects of the simulations are given, followed by several model results in comparison to experimental data.

## 2 The CLOUD-09 chamber

The CLOUD-09 chamber, located at CERN, is a cylindrical stainless steel tank with a height of approx. 4.0 m and a diameter of approx. 3.0 m. The resulting volume of the tank is about 26 m<sup>3</sup>. A schematic diagram of the chamber is shown in Fig. 1.

Different inlets at the bottom, and outlets at the sampling line and top of the tank can be used to connect sampling probes, to put trace gases into the chamber and to evacuate the chamber. Additionally, two fans can be installed inside the chamber to continuously mix the tank's contents. They are located next to the flanges at the top and the bottom (see Figs. 1 and 2). The mixing fans were not housed in the set up investigated here. However, for future experiments hoods around the fans will be used to increase the fan efficiency at low fan speeds. At the top of the tank, there is also an UV-illumination system (illustrated in Fig.6), which is used to trigger the OH production via ozone photolysis. The OH radicals then react with SO<sub>2</sub> to form sulphuric acid (H<sub>2</sub>SO<sub>4</sub>). Dependent on the H<sub>2</sub>SO<sub>4</sub> concentration and on thermodynamic conditions, H<sub>2</sub>SO<sub>4</sub> particle nucleation will occur and can be studied.

The chamber can be exposed to a 3.5 GeV/c positively charged pion ( $\pi^+$ ) beam from a secondary target of the T11 beamline in the East Hall at the CERN PS. This  $\pi^+$  energy is quite close to energies of cosmic ray muons in the lower troposphere. The beam intensity can be varied to yield between about 1 i.p.cm<sup>-3</sup> (no beam) and 10 000 i.p.cm<sup>-3</sup>. For comparison, typical lower tropospheric concentrations are in the order of 1000 i.p.cm<sup>-3</sup>. The ion-pair concentration vs. beam intensity was investigated in Duplissy (2010).

### Numerical simulations of the CLOUD chamber

J. Voigtländer et al.

Title Page

Abstract

Introduction

Conclusions

References

Tables

Figures

◀

▶

◀

▶

Back

Close

Full Screen / Esc

Printer-friendly Version

Interactive Discussion



### 3 Numerical model

#### 3.1 General remarks and numerical grid

An important requirement for the experiments at the CLOUD-09 chamber are well positioned sampling points and a tank's mixing state being as homogeneous as possible. In case of a non well-mixed chamber, the sampling probes may not be representative for the whole tank. To evaluate the experimental configuration, the CLOUD-09 chamber was simulated using the commercially available CFD code FLUENT (ANSYS Inc., Canonsburg, PA, USA) together with the Fine Particle Model (FPM, Wilck et al. (2002), Particle Dynamics GmbH, Leipzig, Germany). The FLUENT model allows the simulation of a wide range of small scale fluid problems, while the FPM was developed for modelling particle dynamical processes. Both models together form the so-called CLOUD-FPM, a model being capable of handling the coupled fluid and particle dynamical processes taking place inside the CLOUD chamber. In CLOUD-FPM, all relevant properties like velocity, temperature, pressure, turbulence parameters, wall losses of the condensable gas phase species and nucleation and growth of ultrafine aerosol particles are treated explicitly.

For the simulations, the geometry of the CLOUD-09 chamber has to be discretised on a numerical grid. Because of the cylindrical geometry of the tank, a 2-D axis-symmetric grid has been used. Compared to a 3-D treatment, such a grid reduces the computational costs significantly. Nevertheless, it is obvious that individual wholes (inlets/outlets) at the chamber bottom/side cannot be simulated using an axis-symmetric grid (bottom: if outside of the tank axis). However, the aim of the current study was to evaluate the tank's mixing state (and not a detailed description of each measuring apparatus probe around the tank), which can be fulfilled by a 2-D grid. Possible effects of such discrete in- and outlets may be studied later on a more detailed 3-D grid.

The flow field inside the chamber is of turbulent nature, even for small flow velocities in the order of few centimetres per second. Therefore, a  $k-\epsilon$ -turbulence-model (Jones and Launder, 1972; Launder and Spalding, 1973) with enhanced wall functions was

## Numerical simulations of the CLOUD chamber

J. Voigtländer et al.

Title Page

Abstract

Introduction

Conclusions

References

Tables

Figures



Back

Close

Full Screen / Esc

Printer-friendly Version

Interactive Discussion



applied for this study. Enhanced wall functions means that a near wall model approach is utilized and the near wall region (laminar boundary layer) has to be resolved by the numerical grid. In more detail, at least 10–20 grid cells within the laminar boundary layer are necessary. The numerical grid used for the simulations shown here has about 20 000 grid cells and was generated matching the requirements of the applied (turbulence) model.

### 3.2 Mixing fans

One of the key parameters in the numerical simulations is a proper description of the mixing fans. Simulations on a 2-D grid do not allow a one to one description of the fans used in the experimental set up (first configuration: 8-blade fans, actually: 4-blade fans). In the model, the mixing fans are treated as zero thickness layers with a pressure jump  $\delta p$  across the layer. Pressure jump and shape of the fans have to be adjusted to experimental data. Two kinds of information were available. These were (a) time dependent measurements of  $\text{H}_2\text{SO}_4$  concentrations of so called  $\text{H}_2\text{SO}_4$  lifetime experiments, and (b) a measured internal radial velocity profile 50 cm above the mixing fan. Both properties were included into the investigations and are discussed in the following. Thereby, it will be shown that the mixing fans have an important influence on the mixing state of the tank.

## 4 Results and discussion

### 4.1 $\text{H}_2\text{SO}_4$ lifetime experiments

#### 4.1.1 Description and experimental data

Due to molecular and turbulent vapour mass diffusion,  $\text{H}_2\text{SO}_4$  is continuously lost to the wall. If there is no additional source, successive  $\text{H}_2\text{SO}_4$  measurements allow to determine the loss of  $\text{H}_2\text{SO}_4$ . For the quasi constant properties characterizing gas

## Numerical simulations of the CLOUD chamber

J. Voigtländer et al.

Title Page

Abstract

Introduction

Conclusions

References

Tables

Figures

◀

▶

◀

▶

Back

Close

Full Screen / Esc

Printer-friendly Version

Interactive Discussion



composition and thermodynamic conditions during one experiment, the vapour diffusion coefficients can be considered as constant. The free parameter in the simulations is the fan speed, influencing the tank's mixing. Its value is fitted to H<sub>2</sub>SO<sub>4</sub> lifetime experiments.

For the H<sub>2</sub>SO<sub>4</sub> lifetime experiments, the chamber was initially fed with the H<sub>2</sub>SO<sub>4</sub> precursor gases (ozone, SO<sub>2</sub> and water vapour). H<sub>2</sub>SO<sub>4</sub> then was produced via ozone photolysis and reaction with SO<sub>2</sub>. Because their concentrations were several orders of magnitude higher than the H<sub>2</sub>SO<sub>4</sub> concentration (10<sup>12</sup> cm<sup>-3</sup> compared to 10<sup>8</sup> cm<sup>-3</sup>), the amount of the precursor gases was quasi constant during the time scale of a typical experiments (several hours). After a certain period of time, H<sub>2</sub>SO<sub>4</sub> production and loss to the wall were in equilibrium, resulting in a quasi constant H<sub>2</sub>SO<sub>4</sub> concentration. Switching off the UV-illumination system again, the H<sub>2</sub>SO<sub>4</sub> production was stopped. The subsequent decrease of H<sub>2</sub>SO<sub>4</sub> due to the transport to the wall loss was recorded via H<sub>2</sub>SO<sub>4</sub> measurements at the sampling points of the tank. The temporal decrease of the H<sub>2</sub>SO<sub>4</sub> concentration for a such an experiment using a 1-fan configuration is shown in Fig. 3 (black line). The x-axis gives the running time and the y-axis the H<sub>2</sub>SO<sub>4</sub> concentration. Thereby, the zero value on the time axis was switched to the beginning of the H<sub>2</sub>SO<sub>4</sub> decrease. Figure 3 shows that, at the sampling volume, the H<sub>2</sub>SO<sub>4</sub> concentration is reduced by 90 percent after 15 min. Short term fluctuations of the H<sub>2</sub>SO<sub>4</sub> concentrations were less than 20 percent. But because of the small sampling volume these are local fluctuations and give no information about the mixing state of the total tank. To evaluate the mixing state, numerical simulations are necessary.

#### 4.1.2 Simulation results

In the CLOUD-FPM simulations, suitable boundary conditions must be chosen. All thermodynamic conditions (e.g. *T*, RH) were adjusted to values equal to those in the experiments (*T* = 291.65 K, RH = 38%). The H<sub>2</sub>SO<sub>4</sub> concentration was prescribed as initial value. Thereby, a homogeneous distribution was assumed. Sources and additional sinks for H<sub>2</sub>SO<sub>4</sub> were excluded.

20019

## Numerical simulations of the CLOUD chamber

J. Voigtländer et al.

Title Page

Abstract

Introduction

Conclusions

References

Tables

Figures

◀

▶

◀

▶

Back

Close

Full Screen / Esc

Printer-friendly Version

Interactive Discussion



Typical concentrations of  $\text{H}_2\text{SO}_4$  in the CLOUD experiments are in the order of  $10^6 \text{ cm}^{-3}$  to  $10^8 \text{ cm}^{-3}$ , corresponding to a  $\text{H}_2\text{SO}_4$  mass in the order of  $10^{-12} \text{ kg}$  up to  $10^{-10} \text{ kg}$  for the whole tank. Due to the small total amount of  $\text{H}_2\text{SO}_4$ , it is a suitable assumption to consider the tank's wall as an infinite sink for  $\text{H}_2\text{SO}_4$ . In the model this was done by defining a  $\text{H}_2\text{SO}_4$  mass fraction of zero at the wall.

Diffusion coefficients needed for the simulations (here:  $\text{H}_2\text{SO}_4$  in air and  $\text{H}_2\text{O}$ ), were taken from literature values. Marti et al. (1997) reported a diffusion coefficient around  $0.1 \text{ cm}^{-3} \text{ s}^{-1}$  for  $\text{H}_2\text{SO}_4$  vapour in  $\text{N}_2$  with a small increase with decreasing relative humidity. Hanson and Eisele (2000) reported RH dependent diffusion coefficients of  $\text{H}_2\text{SO}_4$  in  $\text{N}_2$  and found values around  $0.094 \text{ cm}^2 \text{ s}^{-1}$  at 298 K. However, it was stated in Brus et al. (2010) that diffusion coefficients given by Hanson and Eisele (2000) overestimate experimental data collected in air instead of nitrogen. Therefore,  $\text{H}_2\text{SO}_4$  diffusion in air is supposed to be slower than in  $\text{N}_2$ . Furthermore it was found that diffusion decreases with increasing RH and values of  $0.06 \text{ cm}^2 \text{ s}^{-1}$  were reported for  $\text{H}_2\text{SO}_4$  in  $\text{H}_2\text{O}$  (Hanson and Eisele, 2000). According to these studies, diffusion coefficients of  $0.09 \text{ cm}^2 \text{ s}^{-1}$  ( $\text{H}_2\text{SO}_4$  in air) and  $0.06 \text{ cm}^2 \text{ s}^{-1}$  ( $\text{H}_2\text{SO}_4$  in  $\text{H}_2\text{O}$ ) were applied for simulations shown here.

From the experimental data it is not known whether the tank is well mixed or not. In the simulations the fan was therefore adjusted by a comparison of simulated  $\text{H}_2\text{SO}_4$  concentrations in the assumed sampling volume (at the mid height of the chamber, 20 cm distance to the wall) to the experimental values. Simulation results for the flat disc fan layer with adjusted pressure jump layers compared to the measured  $\text{H}_2\text{SO}_4$  concentrations are shown in Fig. 3 (green line). For a given fan geometry, the calculated  $\text{H}_2\text{SO}_4$  concentration mainly depends on the fan speed. In general, the larger the fan speed, the more  $\text{H}_2\text{SO}_4$  is transported to the wall in a considered time interval.

To evaluate the mixing state, standard deviations of the calculated  $\text{H}_2\text{SO}_4$  concentrations are also included into Fig. 3. The values are volume weighted values calculated for the whole tank and represents a measure for the inhomogeneity in the CLOUD tank.

## Numerical simulations of the CLOUD chamber

J. Voigtländer et al.

Title Page

Abstract

Introduction

Conclusions

References

Tables

Figures

◀

▶

◀

▶

Back

Close

Full Screen / Esc

Printer-friendly Version

Interactive Discussion



The standard deviations were calculated as:

$$\sigma_{\text{H}_2\text{SO}_4} = \sqrt{\frac{\sum_{\text{cell}=1}^N V_{\text{cell}} \left( \rho_{\text{H}_2\text{SO}_4, \text{cell}} - \rho_{\text{H}_2\text{SO}_4, \text{mean}} \right)^2}{\sum_{\text{cell}=1}^N V_{\text{cell}}}} \quad (1)$$

where  $\rho_{\text{H}_2\text{SO}_4, \text{cell}}$  is the  $\text{H}_2\text{SO}_4$  concentration in the actual grid cell and  $\rho_{\text{H}_2\text{SO}_4, \text{mean}}$  is the average  $\text{H}_2\text{SO}_4$  concentration.

Figure 3 shows that simulated standard deviations are about 10 percent of the total  $\text{H}_2\text{SO}_4$  concentration (dark grey area). Furthermore, these 10 percent variation mainly result from the concentration gradient at the wall. This suggests that, with respect to  $\text{H}_2\text{SO}_4$ , the tank is almost well (homogeneously) mixed for this fan configuration. The concentration at the sampling volume almost equals the average value (green dotted line = green solid line). It can be concluded that measured  $\text{H}_2\text{SO}_4$  concentrations are representative for the whole tank and can be compared to simulated average values.

The second input parameter for fitting simulation results to experimental data, a measured internal velocity profile 50 cm above the non housed mixing fan, is shown in Fig. 4 (black dots). The velocity magnitude was measured with a hot-wire anemometer, the flow direction was not measured. Fig. 4 therefore only gives a 1-D profile of the velocity magnitude. The x-axis shows the radial position in the chamber beginning from the center line, and the y-axis is the velocity magnitude. It can be seen that the velocity magnitude is quite low (about  $0.1 \text{ m s}^{-1}$ ) and almost constant over a large part of the measured radial profile. Although measurements of such low velocities may only give an approximate picture of the real conditions, it is obvious from the measurements that a distinctive maximum (jet) above the fan (at the center) was not observed. The profile suggests that the non housed mixing fan used in the CLOUD-09 chamber produces a broad swirl.

With this behaviour, the measured internal velocity profile is in clear contrast to simulation results with flat disc shaped fans (Fig. 4, green line). The simulated profile shows a large velocity maximum (jet) above the fan region. Outside of this region, the velocity

## Numerical simulations of the CLOUD chamber

J. Voigtländer et al.

Title Page

Abstract

Introduction

Conclusions

References

Tables

Figures

◀

▶

◀

▶

Back

Close

Full Screen / Esc

Printer-friendly Version

Interactive Discussion



magnitude falls down to much lower values. The jet above the fan was found independently of the pressure jump settings (velocity magnitude) for this fan geometry. In other words, the measured internal velocity profile could not be reproduced in simulations with such a fan geometry.

To achieve a velocity profile as observed in the experiments (Fig. 4), the shape of the pressure jump fan layers was modified and curved fans were applied in additional simulations (as illustrated in Fig. 5). It is shown in Fig. 4 that internal velocity profiles derived from simulations with such a curved fan may fit the experimental data very well (red line).

The wall loss experiment was also simulated for the arc shaped set up with pressure jump settings adjusted to the experimental velocity profile and also fit the experimental data very well (Fig. 3, red dotted line). On the other hand, such a fan is not suitable to provide a well mixed tank. As shown in Fig. 3, standard deviations of the  $\text{H}_2\text{SO}_4$  concentration are much larger than for the flat fan configuration and goes up to more than 50 percent of the current value (light grey area). Thereby the average  $\text{H}_2\text{SO}_4$  concentration (red solid line) is clearly above the concentration at the sampling volume, indicating that the concentration at the sampling volume is not representative for the whole tank. This means the measured  $\text{H}_2\text{SO}_4$  concentrations cannot be compared to the average values calculated for the whole tank.

In simulations shown above, the  $\text{H}_2\text{SO}_4$  concentration was initially defined. For the further investigations, the production of  $\text{H}_2\text{SO}_4$  in the tank was included into the simulations shown in the following. Because the quasi constant concentrations of the precursor gases, the production rate was also assumed to be constant with respect to time. Also for that reason, the calculation of the chemical reactions was left out of the simulations. In the simulations shown here it was further assumed that the  $\text{H}_2\text{SO}_4$  production only takes place in the (with high intensity) UV-light illuminated part of the tank (Fig. 6, area of red and yellow color). However, a sensitivity study with additional simulations assuming a constant  $\text{H}_2\text{SO}_4$  production rate in the whole tank gave very similar results (for equal total  $\text{H}_2\text{SO}_4$  production) and are therefore not discussed here.

**Numerical  
simulations of the  
CLOUD chamber**

J. Voigtländer et al.

Title Page

Abstract

Introduction

Conclusions

References

Tables

Figures

◀

▶

◀

▶

Back

Close

Full Screen / Esc

Printer-friendly Version

Interactive Discussion



In the experiments, the  $\text{H}_2\text{SO}_4$  concentrations span about 3 orders of magnitude ( $10^6 \text{ cm}^{-3}$ – $10^8 \text{ cm}^{-3}$ ). For that reason,  $\text{H}_2\text{SO}_4$  source rates estimated from the experimental data also vary about 3 orders of magnitude and values in the range between about  $10^4 \text{ cm}^{-3} \text{ s}^{-1}$  and  $10^6 \text{ cm}^{-3} \text{ s}^{-1}$  were found.

In the simulations,  $\text{H}_2\text{SO}_4$  source rates again were adjusted to measured  $\text{H}_2\text{SO}_4$  concentrations and then compared to experimentally determined production rates given above. Simulation results assuming a constant source rate of  $1.5 \times 10^4 \text{ cm}^{-3} \text{ s}^{-1}$  for both fan treatments are exemplarily shown in Fig. 7. The simulated  $\text{H}_2\text{SO}_4$  concentrations agree with the experimental data for both fan settings and a reasonable  $\text{H}_2\text{SO}_4$  source rate within the calculated standard deviation, indicating that the simple approach of a constant  $\text{H}_2\text{SO}_4$  production rate gives proper results.

It can be concluded that both, the flat fan simulation with pressure jump settings adjusted to experimental  $\text{H}_2\text{SO}_4$  wall loss data and also the arc shaped simulation with pressure jump settings fitted to the measured internal velocity profiles, can simulate the observed temporal change of the  $\text{H}_2\text{SO}_4$  concentration during the  $\text{H}_2\text{SO}_4$  lifetime experiments very well. As it can be seen from calculated standard deviations of the  $\text{H}_2\text{SO}_4$  concentration, the first case (flat fan) provides a well mixed tank, while for the second case (arc shaped fan) the  $\text{H}_2\text{SO}_4$  is inhomogeneous distributed over the whole tank.

The measured internal velocity profile could be reproduced only by the arc shaped fan simulation. Although it is obvious that a jet above the mixing fan, as found in the flat fan simulation, was not observed in the measurements, it has to be kept in mind that velocity measurements are very difficult for such low values. From the data discussed here it is therefore not possible to decide whether the flat or the arc shaped fan configuration should be preferred in the the simulations. In the following, both configurations are compared representing the possible extreme cases.

## Numerical simulations of the CLOUD chamber

J. Voigtländer et al.

Title Page

Abstract

Introduction

Conclusions

References

Tables

Figures

◀

▶

◀

▶

Back

Close

Full Screen / Esc

Printer-friendly Version

Interactive Discussion



## 4.2 Cross section profiles

Cross section profiles for flat fan simulation are shown in Fig. 8 (velocity) and Fig. 9 (turbulent intensity). The jet with highest velocity in the region above the fan is clearly visible. The cylindrical region of smaller velocities above the fan hub narrows with increasing distance of the fan. At the top of the tank, the jet dissipates resulting in a (weak) back flow along the wall. In the other regions of the tank, the velocity is very low, but overall the whole tank is captured by the mixing fan (as also found in the  $\text{H}_2\text{SO}_4$  data). According to the velocity profile, highest values of turbulence intensity are found in the shear stress region of the jet, on the fan hub and the wall (Fig. 9). Looking also at the other parts, the overall turbulence intensity is relatively low (mainly below 25%). Furthermore, the influence of the wall is, due to the back flow jet, comparably large. This supports an effective transport towards the wall and reduces the turbulent mixing inside the chamber. Already Schütze and Stratmann (2008) stated that such a 1-fan configuration has, with respect to mixing state and wall impact, drawbacks and should be therefore replaced by a 2-fan configuration with a face to face orientation of the fans.

Cross section profiles for the arc shaped fan configuration are shown in Fig. 8 (velocity) and Fig. 9 (turbulent intensity). The profile differs significantly from those shown in Fig. 8 and Fig. 9. The swirl of the modified mixing fan is much broader, but limited to one half of the tank. In the upper half of the tank the velocity is almost zero and this part is therefore not mixed by the fan. The turbulent intensity (Fig. 11) around the fan is much larger than in Fig. 9, but turbulent mixing is limited to the region next to the fan.

Comparing Figs. 9 and 11 it has to be concluded that, in case of a 1-fan configuration, the mixing of the tank's contents is much better with the jet-like velocity profile of the flat fan configuration.

The results presented here impressively show the impact of the fans on the mixing state, especially for a large tank like the CLOUD chamber. From the given experimental data it has to be concluded that the CLOUD tank may not be homogeneously mixed by a 1-fan configuration. Simulation results with input parameters fitted to the

### Numerical simulations of the CLOUD chamber

J. Voigtländer et al.

Title Page

Abstract

Introduction

Conclusions

References

Tables

Figures



Back

Close

Full Screen / Esc

Printer-friendly Version

Interactive Discussion



experimental data show that the upper half of the tank is not mixed for a 1-fan (arc shaped) configuration. The data suggest that there is an absolutely need for a second mixing fan.

### 4.3 2-fan configuration

To improve the mixing inside the tank, a second fan has been already installed in the CLOUD-09 chamber for actual and further studies. Therefore, simulation results for a 2-fan configuration were also carried out. The pressure jump settings for the second fan were adjusted to the same values as fitted for the first fan. The profiles are not shown here separately, but in such a 2-fan configuration, the whole tank is well mixed for both, flat and an arc shaped mixing fans. Due to the second mixing fan and equal pressure jump properties than for the 1-fan configuration,  $\text{H}_2\text{SO}_4$  wall loss and production rates are increased and standard deviations of the  $\text{H}_2\text{SO}_4$  concentration are much smaller than for the 1-fan configuration, indicating a well mixed tank.

### 4.4 Mixing of the CLOUD tank's contents

Time resolved simulations were carried out to estimate time scales for mixing the tank's contents. In more detail, the response of the system to an instantaneous change of (a) the wall temperature by 20 K (291.65 to 271.65 K), and (b) the water mass fraction at the wall by 0.015 (0.05 to 0.20) was investigated. Simulations were performed for both, the one and the two fan configuration. The fan settings (1 or 2 fans, fan shape, pressure jump settings) were the same as for the  $\text{H}_2\text{SO}_4$  lifetime experiments described above.

Simulation results of the temperature jump simulation are shown in Fig. 12. Dependent on the fan configuration, the corresponding mixing times to reduce the difference between wall and tank's average value to  $1/e$  of the initial value, called  $1/e$  time in the following, are between about 100 s and 220 s. For the flat fan set up, the addition of a second fan has only a small influence, because the 1-fan configuration already provides a well mixed tank. A similar behaviour was already found in Schütze and Stratmann

## Numerical simulations of the CLOUD chamber

J. Voigtländer et al.

Title Page

Abstract

Introduction

Conclusions

References

Tables

Figures



Back

Close

Full Screen / Esc

Printer-friendly Version

Interactive Discussion



(2008). In contrast, a second fan decreases the mixing time by a factor of more than 2 for the arc shaped fan configuration. Because of the effective turbulent mixing, the arc shaped 2-fan configuration has the smallest 1/e mixing time of all configurations investigated here with a value of approx. 100 s.

5 Similar as given for the  $\text{H}_2\text{SO}_4$  concentration, a measure for the inhomogeneity in the tank is the volume-averaged deviation of  $T_{\text{mean}}$  given by:

$$\Delta\bar{T} = \sqrt{\frac{\sum_{\text{cell}=1}^N V_{\text{cell}} (T_{\text{cell}} - T_{\text{mean}})^2}{\sum_{\text{cell}=1}^N V_{\text{cell}}}} \quad (2)$$

where cell is the cell index,  $V_{\text{cell}}$  is cell volume and  $T_{\text{cell}}$  is cell temperature.

10 The volume-averaged deviation of  $T_{\text{mean}}$  is exemplarily shown for the arc shaped (1 fan) configuration in Fig.12b. The  $dT_{\text{mean}}$  value is zero in the beginning. This is due to the homogeneous tank in the beginning of the time-dependent simulations. Caused by the temperature change of the wall, it increases rapidly. After reaching a maximum value it decreases slowly back to zero for long time scales. The inhomogeneity of the tank is significantly reduced, if a second fan is installed ( $\Delta T_{\text{mean}}$  reduced). Again it is obvious that the usage of only 1-fan (arc shaped) is not suitable to provide a well mixed tank.

15 Mixing time scales for heat and mass transport processes were found to be very similar. The 1/e-times for a instantaneous jump of the water mass fraction at the wall are almost identical to the 1/e-times for a temperature jump (around 180 s) for the flat fan. Therefore, the results are not plotted again.

20 In summary it can be concluded that typical mixing times for the CLOUD tank are in the range of few minutes.

## Numerical simulations of the CLOUD chamber

J. Voigtländer et al.

Title Page

Abstract

Introduction

Conclusions

References

Tables

Figures

⏪

⏩

◀

▶

Back

Close

Full Screen / Esc

Printer-friendly Version

Interactive Discussion



## 4.5 Simulation of particle nucleation and growth

Time dependent CLOUD-FPM calculations were also carried out to simulate the nucleation and growth of  $\text{H}_2\text{SO}_4$  -  $\text{H}_2\text{O}$  particles in the CLOUD tank. Simulations again were performed for different fan configurations. The focus was on the investigation of the mixing state and not a quantitative theoretical description of the experiments. For that reason, aspects of ion induced nucleation or additional condensing gases (beside  $\text{H}_2\text{SO}_4$ ), as supposed in Duplissy (2010), were not considered.

The simulations were similar to the simulations shown above, except that the simulation of particle dynamic processes were additionally switched on. At time  $t = 0$ , the particle concentration was set to zero. Particles were generated by nucleation from  $\text{H}_2\text{SO}_4$  vapour produced in the chamber. Therefore, a parametrization of the  $\text{H}_2\text{SO}_4$  vapour dependent nucleation rate and the subsequent particle growth has to be included into the model. With respect to the computational effort, classical nucleation theory is very expensive. Simplified parametrisations of nucleation rate  $J$  are based on the equation:

$$J = K \cdot [\text{conc}]^A \quad (3)$$

with the concentration of the considered nucleating vapour [conc], and the fitting parameters  $K$  (kinetic coefficient) and  $A$  (exponential term), derived from experiments (e.g., Berndt et al., 2006). Values of  $A = [1..2]$  were found to give the best results. For example, Kulmala et al. (2004) presented a so called cluster activation theory, using a value of  $A = 1$ , resulting in  $K$  values between  $10^{-7}$  and  $10^{-5} \text{ s}^{-1}$  (Sihto et al., 2006; Riipinen et al., 2007). McMurry (1980) presented a collision-controlled kinetic nucleation parametrization with an exponential coefficient of  $A = 2$ . Therewith, ambient data give results of  $K$  between  $10^{-14}$  and  $10^{-11} \text{ cm}^{-3} \text{ s}^{-1}$  (Sihto et al., 2006; Riipinen et al., 2007; Kuang et al., 2008). The different nucleation theories are compared in Herrmann et al. (2010). They differ, dependent on the conditions (RH,  $\text{H}_2\text{SO}_4$  concentration), by several orders of magnitude. Ion induced nucleation, investigated in the CLOUD-09 chamber, is a special issue. But as results presented here only want (a) to show the

20027

ACPD

11, 20013–20049, 2011

### Numerical simulations of the CLOUD chamber

J. Voigtländer et al.

Title Page

Abstract

Introduction

Conclusions

References

Tables

Figures

◀

▶

◀

▶

Back

Close

Full Screen / Esc

Printer-friendly Version

Interactive Discussion



feasibility of the model to simulate such particle nucleation events and (b) to investigate the the spatial and temporal inhomogeneity of the particle number size distribution, the simple parametrization according to McMurry (1980) was applied for the simulation shown here.

Particle growth of the freshly nucleated particles was described by a simple growth law given by Seinfeld and Pandis (1997). Applying this growth law, there is no kinetic description of the particle growth with respect to water. This means, concerning water the particles are always assumed to be in thermodynamical equilibrium. The growth law is given by:

$$\frac{dD_p}{dT} = \frac{M_s \bar{c} \alpha (C_{\text{vap}} - C_{\text{eq}})}{2\rho} \text{WR} \quad (4)$$

where  $D_p$  is particle diameter,  $\rho$  is particle density,  $M_s$  is molar weight of  $\text{H}_2\text{SO}_4$ ,  $\bar{c}$  is the mean molecular velocity of  $\text{H}_2\text{SO}_4$  (assumed as  $333 \text{ m s}^{-1}$ ),  $\alpha$  is the mass transfer accommodation coefficient (assumed to be 1),  $C_{\text{vap}}$  is the  $\text{H}_2\text{SO}_4$  concentration,  $C_{\text{eq}}$  is the equilibrium concentration of  $\text{H}_2\text{SO}_4$  (assumed to be zero here), and WR is the ratio of wet to dry particle diameter (dry: only  $\text{H}_2\text{SO}_4$ ). Neglecting the Kelvin term, this ratio only depends on RH.

WR was calculated by a linear fitting equation according to vapour pressure values given in Tabazadeh et al. (1997). In the FPM model, the particle number size distribution was described by a single mode log-normal distribution.

The simulation shown here was done for a 2 arc shaped fan configuration. Considering the particle growth by  $\text{H}_2\text{SO}_4$  only, concentrations in the order of  $10^6$  to  $10^7 \text{ cm}^{-3}$ , as considered here, would result in growth rates smaller than  $1 \text{ nm h}^{-1}$  (Duplissy, 2010; Nieminen et al., 2010). It was therefore speculated in Duplissy (2010) that experimental determined growth rates up to about  $40 \text{ nm h}^{-1}$  were caused by additional, unidentified condensable vapours. In the CLOUD-FPM simulations, only  $\text{H}_2\text{SO}_4$  was considered. For comparable growth rates (Fig. 15), a  $\text{H}_2\text{SO}_4$  production rate of  $2.5 \times 10^6 \text{ cm}^{-3} \text{ s}^{-1}$  was assumed in the numerical simulation, resulting in a maximum  $\text{H}_2\text{SO}_4$  concentration

## Numerical simulations of the CLOUD chamber

J. Voigtländer et al.

Title Page

Abstract

Introduction

Conclusions

References

Tables

Figures

◀

▶

◀

▶

Back

Close

Full Screen / Esc

Printer-friendly Version

Interactive Discussion



## Numerical simulations of the CLOUD chamber

J. Voigtländer et al.

Title Page

Abstract

Introduction

Conclusions

References

Tables

Figures

⏪

⏩

◀

▶

Back

Close

Full Screen / Esc

Printer-friendly Version

Interactive Discussion



of about  $5 \times 10^8 / \text{cm}^{-3}$  (see Fig. 13). Due to the high  $\text{H}_2\text{SO}_4$  concentration, a very small nucleation rate coefficient of  $K = 2.5 \times 10^{-17}$  was applied to limit particle nucleation rate and total particle number. Applying this value, the particle nucleation rate was up to about  $6 \text{ cm}^{-3} \text{ s}^{-3}$  (Fig. 14), which is in the range of the formation rates determined in the experiments ( $0.1$  to  $100 \text{ cm}^{-3} \text{ s}^{-1}$ , Duplissy, 2010). As shown by the included (small) standard deviation of the particle number (Fig. 14), the particles were also found to be quite homogeneously distributed over the tank's volume for this fan configuration. Furthermore, mean particle size and sigma of the log-normal distribution are also almost constant in the whole tank. Thus, the tank can be considered quite well mixed also for the freshly nucleated  $\text{H}_2\text{SO}_4$  particles, if a suitable fan configuration, as given by the 2-fan set-up, is applied.

Again, the results are different for an arc shaped 1-fan configuration, as such a set up cannot provide well mixed conditions inside the tank.

In summary, the mixing state of the particle number size distribution with fresh nucleated small particles was found to be very similar to the mixing state of the gas species. This means, if the tank's gas contents are well mixed, the nano-sized particles are also homogeneously distributed over the whole tank.

## 5 Conclusions

The CLOUD-FPM model was applied to conduct numerical simulations of the CLOUD tank ( $26 \text{ m}^3$ ) established at CERN (Switzerland). In the model, the CLOUD-09 chamber was described by a 2-D axis-symmetric grid. The simulations were applied to calculate the coupled fields of temperature, saturation ratio, flow velocity, vapour species and particle number size distribution.

The description of the mixing fans were realized via polynomial pressure jump settings at zero thickness layers. The settings for the fans were derived by a comparison of calculated with measured  $\text{H}_2\text{SO}_4$  concentrations and a measured velocity profile. It was shown that the mixing state largely depends on the characteristics of the fans.

---

**Numerical  
simulations of the  
CLOUD chamber**J. Voigtländer et al.

---

[Title Page](#)[Abstract](#)[Introduction](#)[Conclusions](#)[References](#)[Tables](#)[Figures](#)[⏪](#)[⏩](#)[◀](#)[▶](#)[Back](#)[Close](#)[Full Screen / Esc](#)[Printer-friendly Version](#)[Interactive Discussion](#)

Applying flat fans,  $\text{H}_2\text{SO}_4$  can be assumed to be homogeneously distributed over the whole volume of the tank also for a 1-fan configuration. For this configuration, maximum volume-averaged deviations from the mean were about 10 % of the total  $\text{H}_2\text{SO}_4$  concentration. On the other hand, calculated and measured internal velocity profile are not in agreement for a fan with such a characteristics. Changing the fan shape to arc fit experimental and simulated data, but such a fan is not suitable to mix the whole tank, as indicated by the resulting large variations of the ( $\text{H}_2\text{SO}_4$ ) concentration inside the chamber. It was found that there is an absolute need for a second fan in such a set up. Therefore, a second fan has been already installed in the CLOUD chamber for actual and further experiments.

With fitted fan speed settings, the  $\text{H}_2\text{SO}_4$  cycle in the tank was also simulated. Assuming constant  $\text{H}_2\text{SO}_4$  production rates in a certain, by the UV system illuminated part of the tank, the increase of the  $\text{H}_2\text{SO}_4$  concentration up to an equilibrium concentration was simulated. Simulation results agree well with the experimental data for both fan shapes and reasonable  $\text{H}_2\text{SO}_4$  production rates.

The 1/e-mixing times for the system response to a instantaneous change of the wall temperature or water saturation ratio were found to be in the range of few minutes. Again, a second fan significantly reduces the standard deviations and, depending on the fan characteristics, it also may decreases the mixing time by a factor of 2–3.

Particles were also included into the simulations. It was found that the mixing state of the particle number size distribution properties is quite similar to the mixing state of the gaseous components. In other words, if the tank is homogeneously mixed with respect to  $\text{H}_2\text{SO}_4$ , it can be also considered well mixed with respect to the fresh nucleated nano-sized particles. In turn, using a mixing fan as given by the arc shaped layer does not allow to distribute the particles homogeneously over the whole tank.

In conclusion, only 2 mixing fans can guarantee well mixed conditions inside the chamber. A configuration with only 1 fan comparable to the arc shaped fan investigated here is not suitable to mix the whole tank properly. In fact, the second half of the tank is not mixed by such a fan. A jet producing fan, e.g. reached by a hood around the fan,

## Numerical simulations of the CLOUD chamber

J. Voigtländer et al.

Title Page

Abstract

Introduction

Conclusions

References

Tables

Figures

◀

▶

◀

▶

Back

Close

Full Screen / Esc

Printer-friendly Version

Interactive Discussion



can mix the whole tank (10 % standard deviations), but the influence of the wall is large in such a configuration. It follows that the position of the sampling point is a critical issue in such a set up. Installing a second fan, the chamber can be assumed to be homogeneously mixed with respect to gaseous and particle properties of the freshly nucleated nano-sized particles for both fan shapes investigated here. For the 2-fan configuration, the characteristics of the fans and the positions of the sampling points (located at about half of the height) are therefore much less critical.

Results shown here were carried out for a tank with the geometry of the CLOUD-09 chamber. However as stated in this paper, the results largely agree with similar studies made for a smaller cloud tank (Schütze and Stratmann, 2008). Therefore, investigations shown here should be also valid for similar cloud tanks. This means, an at least 2-fan configuration should be chosen to provide well mixed conditions inside of such a chamber.

*Acknowledgements.* We would like to thank CERN for supporting CLOUD with important technical resources, for providing a particle beam from the CERN Proton Synchrotron, and the German Federal Ministry of Education and Research (BMWF) for founding the modelling research presented here (project no. 01LK0902B).

## References

- Berndt, T., Böge, O., and Stratmann, F.: Formation of atmospheric  $\text{H}_2\text{SO}_4/\text{H}_2\text{O}$  particles in the absence of organics: A laboratory study, *Geophys. Res. Lett.*, 33(L15817), 2006. 20027
- Brus, D., Hyvärinen, A.-P., Viisanen, Y., Kulmala, M., and Lihavainen, H.: Homogeneous nucleation of sulfuric acid and water mixture: experimental setup and first results, *Atmos. Chem. Phys.*, 10, 2631–2641, doi:10.5194/acp-10-2631-2010, 2010. 20020
- Carlslaw, K., Harrison, R., and Kirkby, J.: Cosmic rays, clouds, and climate, *Science*, 298, 1732–1737, 2002. 20015
- Duplissy, J., Enghoff, M. B., Aplin, K. L., Arnold, F., Aufmhoff, H., Avngaard, M., Baltensperger, U., Bondo, T., Bingham, R., Carlslaw, K., Curtius, J., David, A., Fastrup, B., Gagn, S., Hahn, F., Harrison, R. G., Kellett, B., Kirkby, J., Kulmala, M., Laakso, L., Laaksonen, A., Lillestol, E.,

## Numerical simulations of the CLOUD chamber

J. Voigtländer et al.

Title Page

Abstract

Introduction

Conclusions

References

Tables

Figures

◀

▶

◀

▶

Back

Close

Full Screen / Esc

Printer-friendly Version

Interactive Discussion



Lockwood, M., Mkel, J., Makhmutov, V., Marsh, N. D., Nieminen, T., Onnela, A., Pedersen, E., Pedersen, J. O. P., Polny, J., Reichl, U., Seinfeld, J. H., Sipil, M., Stozhkov, Y., Stratmann, F., Svensmark, H., Svensmark, J., Veenhof, R., Verheggen, B., Viisanen, Y., Wagner, P. E., Wehrle, G., Weingartner, E., Wex, H., Wilhelmsson, M., and Winkler, P. M.: Results from the CERN pilot CLOUD experiment, *Atmos. Chem. Phys.*, 10, 1635–1647, doi:10.5194/acp-10-1635-2010, 2010. 20015, 20016, 20027, 20028, 20029

Hanson, D. and Eisele, F.: Diffusion of  $\text{H}_2\text{SO}_4$  in humidified nitrogen: Hydrated  $\text{H}_2\text{SO}_4$ , *J. Phys. Chem. A*, 104, 1715–1719, 2000. 20020

Herrmann, E., Brus, D., Hyvärinen, A.-P., Stratmann, F., Wilck, M., Lihavainen, H., and Kulmala, M.: A computational fluid dynamics approach to nucleation in the water-sulfuric acid-system, *J. Phys. Chem.*, 114(31), 8033–8042, 2010. 20027

IPCC2007, *Climate change 2007*, Tech. rep., Cambridge University Press., 2007. 20014

Jones, W. and Launder, B.: The prediction of laminarization with a two-equation model of turbulence, *Int J. Heat Mass Transfer*, 15, 301–314, 1972. 20017

Kuang, C., McMurry, P., McCormick, A., and Eisele, F.: Dependence of nucleation rates on sulfuric acid vapor concentration in diverse atmospheric locations., *J. Geophys. Res.*, 113(D10209), 2008. 20027

Kulmala, M., Vehkamäki, H., Petäjä, T., DalMaso, M., Lauri, A., Kerminen, V.-M., Birmili, W., and McMurry, P.: Formation and growth rates of ultrafine atmospheric particles: a review of observations, *J. Aerosol Sci.*, 35, 143–176, 2004. 20027

Launder, B. and Spalding, D.: The numerical computation of turbulent flows, *Comput. Method. Appl. M.*, 3(2), 269–289, 1973. 20017

Marti, J., Jefferson, A., PingCai, X., Richert, C., McMurry, P., and Eisele, F.:  $\text{H}_2\text{SO}_4$  vapor pressure of sulfuric acid and ammonium sulfate solutions, *J. Geophys. Res.*, 102(D3), 3725–3735, 1997. 20020

McMurry, P.: Photochemical aerosol formation from  $\text{SO}_2$ : A theoretical analysis of smog chamber data, *J. Colloid Interface Sci.*, 78, 513–527, 1980. 20027, 20028

Nieminen, T., Lehtinen, K. E. J., and Kulmala, M.: Sub-10 nm particle growth by vapor condensation - effects of vapor molecule size and particle thermal speed, *Atmos. Chem. Phys.*, 10, 9773–9779, doi:10.5194/acp-10-9773-2010, 2010. 20028

Riipinen, I., Sihto, S.-L., Kulmala, M., Arnold, F., Dal Maso, M., Birmili, W., Saarnio, K., Teiniälä, K., Kerminen, V.-M., Laaksonen, A., and Lehtinen, K. E. J.: Connections between atmospheric sulphuric acid and new particle formation during QUEST IIIIV campaigns in Heidel-

---

**Numerical  
simulations of the  
CLOUD chamber**J. Voigtländer et al.

---

[Title Page](#)[Abstract](#)[Introduction](#)[Conclusions](#)[References](#)[Tables](#)[Figures](#)[⏪](#)[⏩](#)[◀](#)[▶](#)[Back](#)[Close](#)[Full Screen / Esc](#)[Printer-friendly Version](#)[Interactive Discussion](#)

berg and Hyytiälä, Atmos. Chem. Phys., 7, 1899–1914, doi:10.5194/acp-7-1899-2007, 2007.  
20027

Schütze, M. and Stratmann, F.: Numerical simulation of cloud droplet formation in a tank,  
Comput. Geosci., 34, 1034–1043, 2008. 20015, 20024, 20025, 20031

5 Seinfeld, J. and Pandis, S.: Atmospheric Chemistry and Physics: From air pollution to climate  
change, Wiley, New York, USA, 1997. 20028

Sihto, S.-L., Kulmala, M., Kerminen, V.-M., Dal Maso, M., Petaäjä, T., Riipinen, I., Korhonen, H.,  
Arnold, F., Janson, R., Boy, M., Laaksonen, A., and Lehtinen, K. E. J.: Atmospheric sulphuric  
10 acid and aerosol formation: implications from atmospheric measurements for nucleation and  
early growth mechanisms, Atmos. Chem. Phys., 6, 4079–4091, doi:10.5194/acp-6-4079-  
2006, 2006. 20027

Svensmark, H. and Friis-Christensen, E.: Variation of cosmic ray flux and global cloud cover-  
age - a missing link in solar-climate relationships, J. Atm. Sol. Terr. Phys., 59, 1225–1232,  
1997. 20015

15 Tabazadeh, A., Toon, O., Clegg, S., and Hamill, P.: A new parameterization of H<sub>2</sub>SO<sub>4</sub>/H<sub>2</sub>O  
aerosol composition: Atmospheric implications, Geophys. Res. Lett., 24(15), 1931–1934,  
1997. 20028

Wilck, M., Stratmann, F., and Whitby, E.: A fine particle model for fluent: Description and  
application, in Proc. Sixth Int. Aerosol Conf., pp. 1269–1270, Chinese Association for Aerosol  
20 Research in Taiwan/International Aerosol Research Assembly, Taipei, Taiwan, 2002. 20017

## Numerical simulations of the CLOUD chamber

J. Voigtländer et al.

**Table 1.** The effect of different fan configurations on tank mixing.

Configuration	$T_{\text{wall}}$		$X_{\text{H}_2\text{O, wall}}$	
	291.65 K→271.65 K		0.005→0.02	
	$t_{/e}[s]$	$\Delta\bar{T}_{\text{max}}[K]$	$t_{\text{max}}[s]$	$t_{/e}[s]$
1 x fan (flat)	184	1.88	45	
2 x fan (flat)	151	1.61	8	
1 x fan (arc)	222	3.03	282	287
2 x fan (arc)	100	2.00	21	118

Title Page

Abstract

Introduction

Conclusions

References

Tables

Figures

◀

▶

◀

▶

Back

Close

Full Screen / Esc

Printer-friendly Version

Interactive Discussion



**Numerical  
simulations of the  
CLOUD chamber**

J. Voigtländer et al.

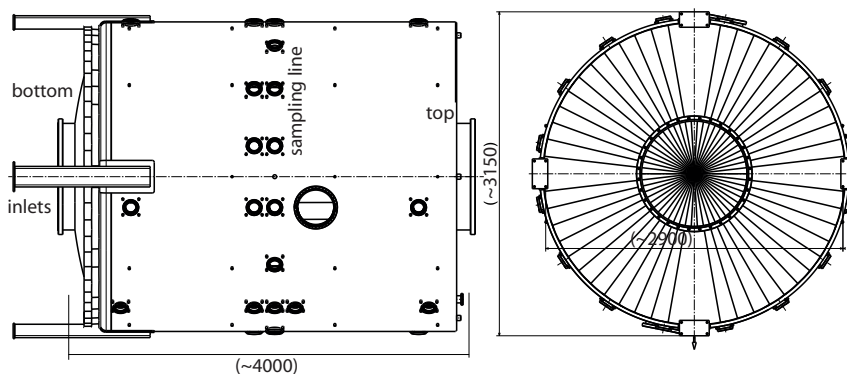


**Fig. 1.** Schematic diagram of the CLOUD-09 chamber, a cloud tank with  $\approx 26 \text{ m}^3$ . According to the figures shown in the following, the front view of the tank was rotated by  $90^\circ$  (clockwise). At the mid-height, the wholes to take of the sampling probes (sampling line) are visible.

[Title Page](#)[Abstract](#)[Introduction](#)[Conclusions](#)[References](#)[Tables](#)[Figures](#)[◀](#)[▶](#)[◀](#)[▶](#)[Back](#)[Close](#)[Full Screen / Esc](#)[Printer-friendly Version](#)[Interactive Discussion](#)

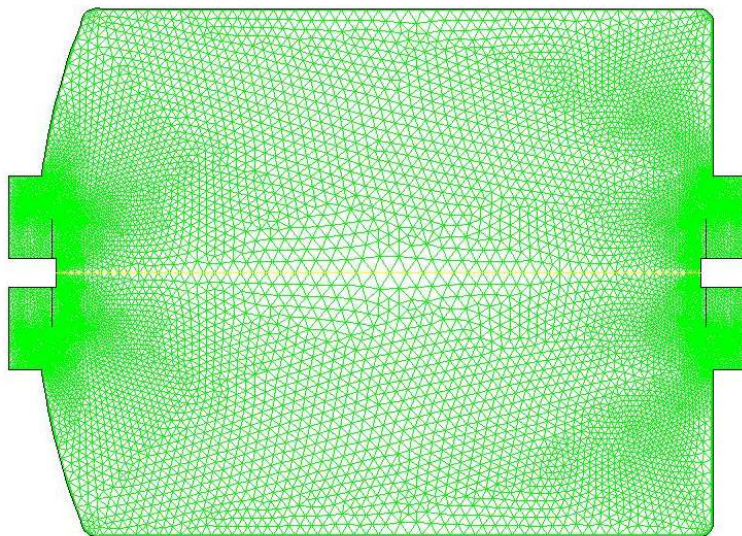


**Fig. 2.** Numerical grid used for the CLOUD-FPM simulations. The thin lines next to the bottom and the top are representing the mixing fans and the small, not meshed areas in between are the fan hubs.

**Numerical simulations of the CLOUD chamber**

J. Voigtländer et al.

Title Page

Abstract

Introduction

Conclusions

References

Tables

Figures

◀

▶

◀

▶

Back

Close

Full Screen / Esc

Printer-friendly Version

Interactive Discussion



**Numerical  
simulations of the  
CLOUD chamber**

J. Voigtländer et al.

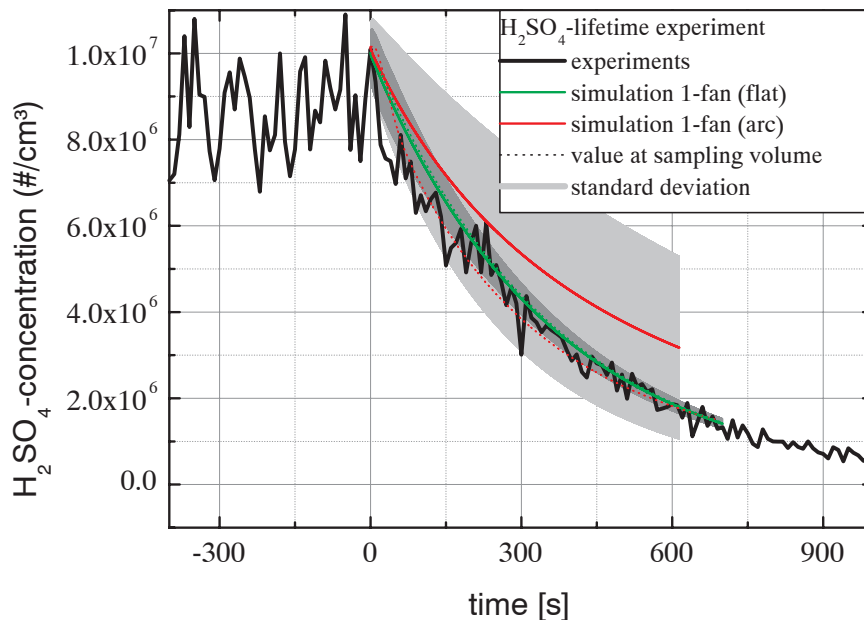


**Fig. 3.**  $\text{H}_2\text{SO}_4$  lifetime experiments compared to numerical simulations. The experiment was RUN 12 at 25 November 2009. The simulations were performed for a 1-fan configuration. The green line shows the results for a flat fan geometry. The red line gives the results for the arc shaped fan configuration. The dotted lines are the results at the assumed sampling spot, the solid lines are calculated volume weighted average values. The gray areas standard deviations, calculated for the average values.

[Title Page](#)[Abstract](#)[Introduction](#)[Conclusions](#)[References](#)[Tables](#)[Figures](#)[◀](#)[▶](#)[◀](#)[▶](#)[Back](#)[Close](#)[Full Screen / Esc](#)[Printer-friendly Version](#)[Interactive Discussion](#)

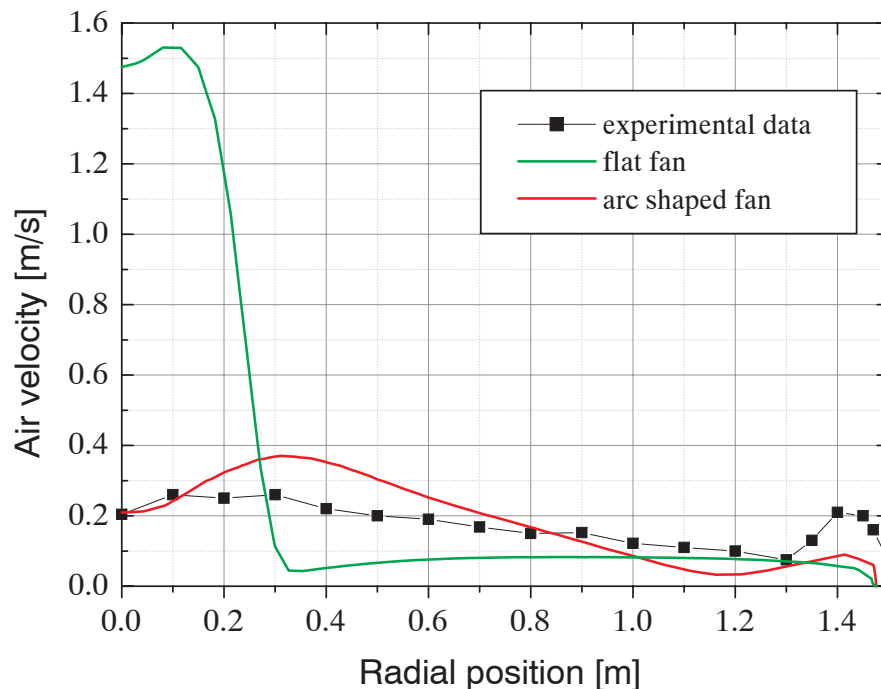


**Fig. 4.** Measured internal air velocity 50 cm above the fan (black dots) compared to simulation results. The flow direction was not measured, but properly has large azimuthal and radial components, especially in the outer region. There was always no hood around the fan. Different shapes of the zero thickness pressure jump layer (representing the mixing fan) results in different velocity profiles. A flat fan configuration result in a velocity profile significantly different from experimental data (green line). To match the experimental data, arc shaped layers are necessary (red line).

**Numerical simulations of the CLOUD chamber**

J. Voigtländer et al.

Title Page

Abstract Introduction

Conclusions References

Tables Figures

⏪ ⏩

◀ ▶

Back Close

Full Screen / Esc

Printer-friendly Version

Interactive Discussion



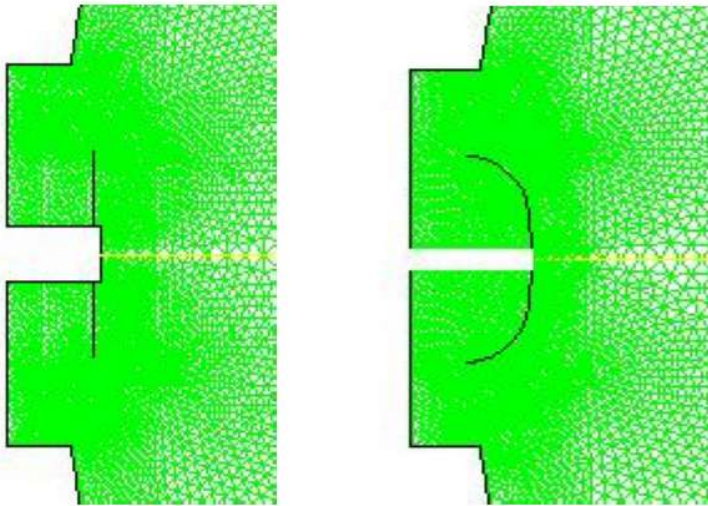


**Fig. 5.** Part of the numerical grid to show the different fan shape treatments.

**Numerical simulations of the CLOUD chamber**

J. Voigtländer et al.

Title Page

Abstract

Introduction

Conclusions

References

Tables

Figures

◀

▶

◀

▶

Back

Close

Full Screen / Esc

Printer-friendly Version

Interactive Discussion



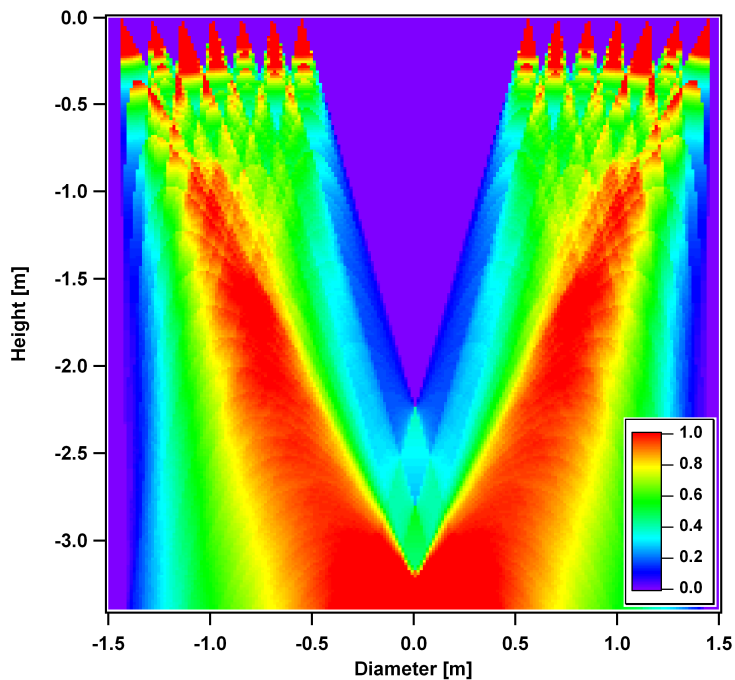


**Fig. 6.** UV Illumination below 317 nm inside the CLOUD-09 chamber. Set up with 7 feedthrough rings (before 2011).

**Numerical simulations of the CLOUD chamber**

J. Voigtländer et al.

Title Page

Abstract Introduction

Conclusions References

Tables Figures

◀ ▶

◀ ▶

Back Close

Full Screen / Esc

Printer-friendly Version

Interactive Discussion



**Numerical  
simulations of the  
CLOUD chamber**

J. Voigtländer et al.

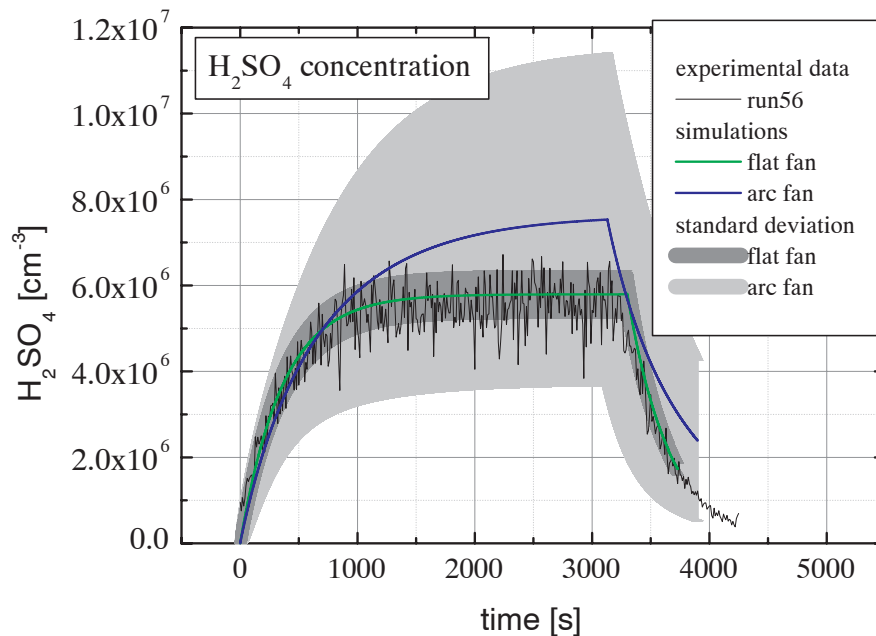


**Fig. 7.** Calculated H<sub>2</sub>SO<sub>4</sub> concentration with constant H<sub>2</sub>SO<sub>4</sub> production rate in comparison to experimental CLOUD data. The source rate was  $1.5 \times 10^4 \text{ cm}^{-3} \text{ s}^{-1}$ .

Title Page

Abstract

Introduction

Conclusions

References

Tables

Figures

◀

▶

◀

▶

Back

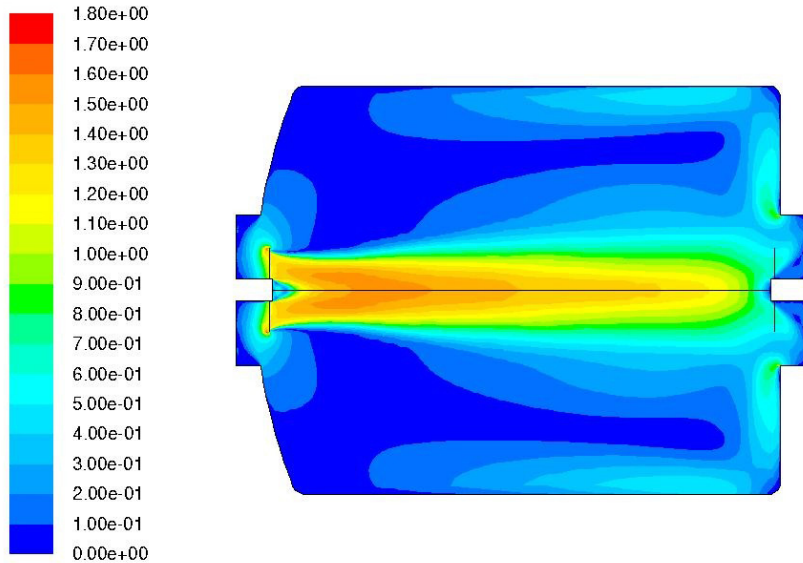
Close

Full Screen / Esc

Printer-friendly Version

Interactive Discussion





Contours of Velocity Magnitude (m/s)

**Fig. 8.** Example of simulation results of the CLOUD-09 chamber using a 1-fan configuration. The figure shows the velocity magnitude for a flat fan configuration.

**Numerical simulations of the CLOUD chamber**

J. Voigtländer et al.

Title Page

Abstract Introduction

Conclusions References

Tables Figures

◀ ▶

◀ ▶

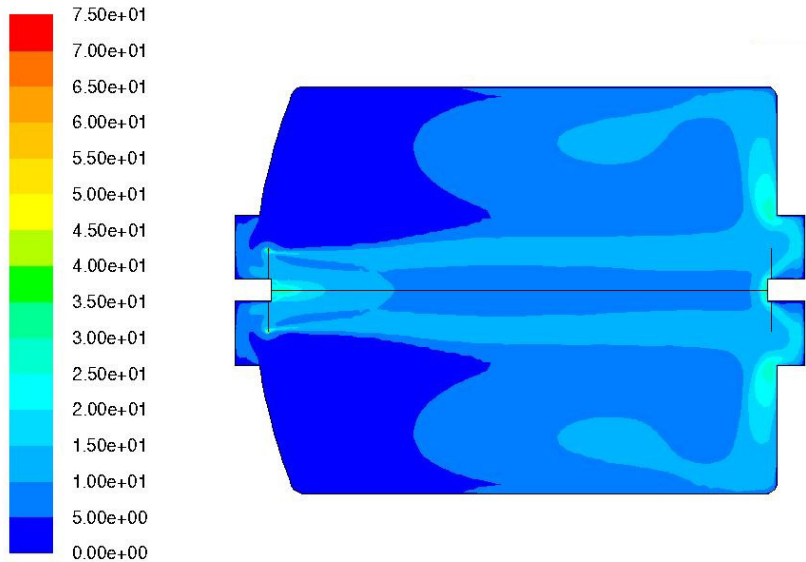
Back Close

Full Screen / Esc

Printer-friendly Version

Interactive Discussion





Contours of Turbulent Intensity (%)

**Fig. 9.** Example of simulation results of the CLOUD-09 chamber using a 1-fan configuration. The figure shows the turbulent intensity for a flat fan configuration.

**Numerical simulations of the CLOUD chamber**

J. Voigtländer et al.

Title Page

Abstract Introduction

Conclusions References

Tables Figures

◀ ▶

◀ ▶

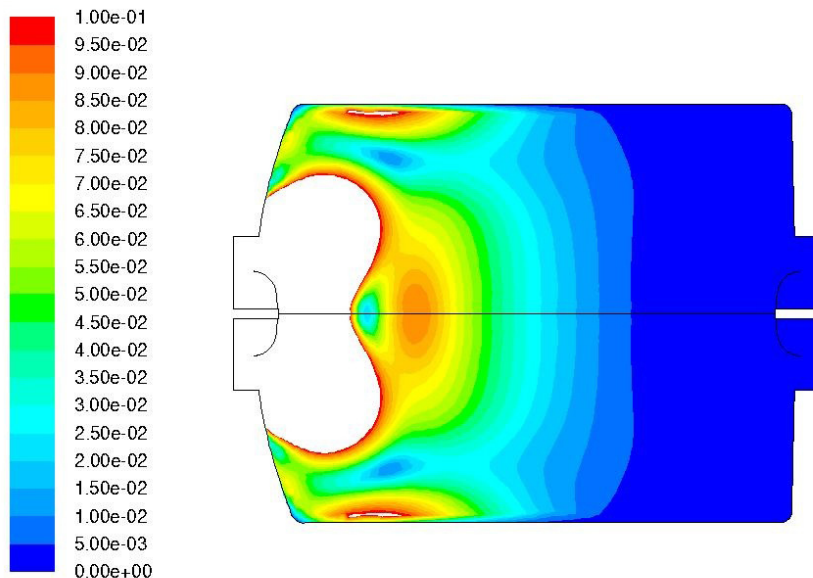
Back Close

Full Screen / Esc

Printer-friendly Version

Interactive Discussion





Contours of Velocity Magnitude (m/s)

**Fig. 10.** Example of simulation results of the CLOUD-09 chamber using a 1-fan configuration. The figure shows the velocity magnitude for a curved fan configuration.

**Numerical simulations of the CLOUD chamber**

J. Voigtländer et al.

Title Page

Abstract Introduction

Conclusions References

Tables Figures

◀ ▶

◀ ▶

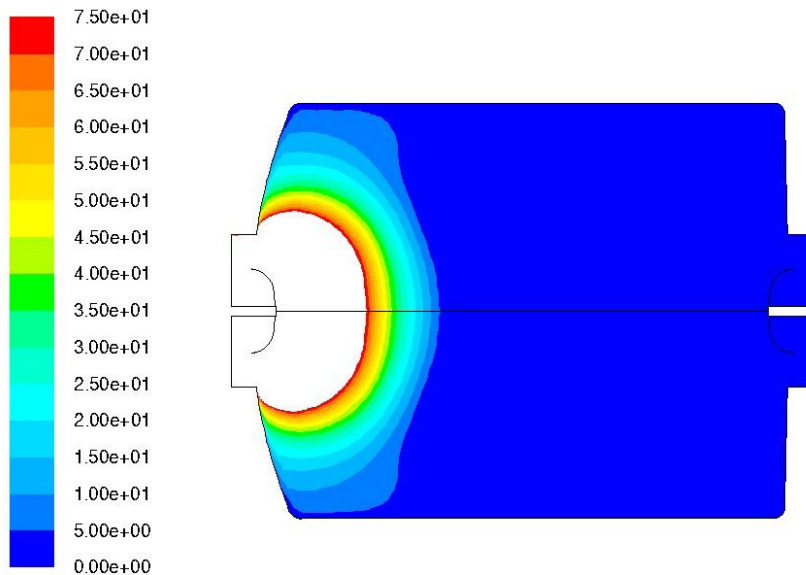
Back Close

Full Screen / Esc

Printer-friendly Version

Interactive Discussion





Contours of Turbulent Intensity (%)

**Fig. 11.** Example of simulation results of the CLOUD-09 chamber using a 1-fan configuration. The figure shows the turbulent intensity for a curved fan configuration.

**Numerical simulations of the CLOUD chamber**

J. Voigtländer et al.

Title Page

Abstract Introduction

Conclusions References

Tables Figures

◀ ▶

◀ ▶

Back Close

Full Screen / Esc

Printer-friendly Version

Interactive Discussion



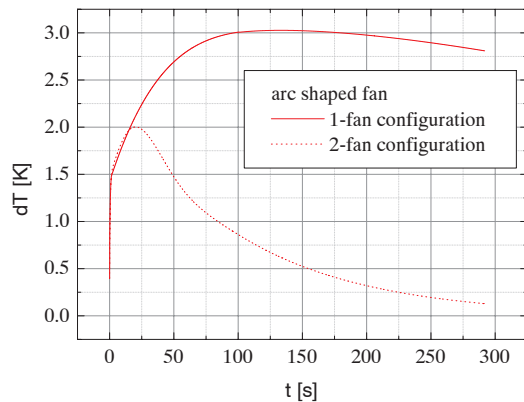
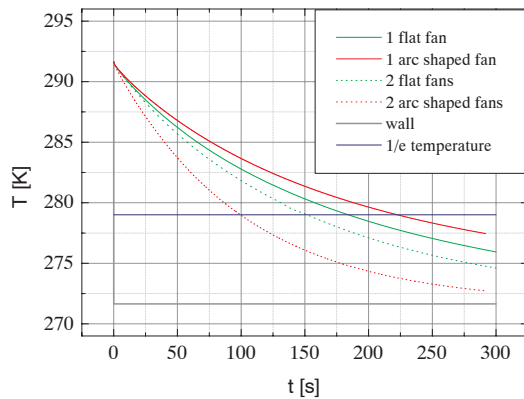


**Fig. 12.** Temporal development of  $T$  and  $\delta T$  for an instantaneous drop of wall temperature by 20 K.

**Numerical simulations of the CLOUD chamber**

J. Voigtländer et al.

Title Page

Abstract Introduction

Conclusions References

Tables Figures

⏪ ⏩

◀ ▶

Back Close

Full Screen / Esc

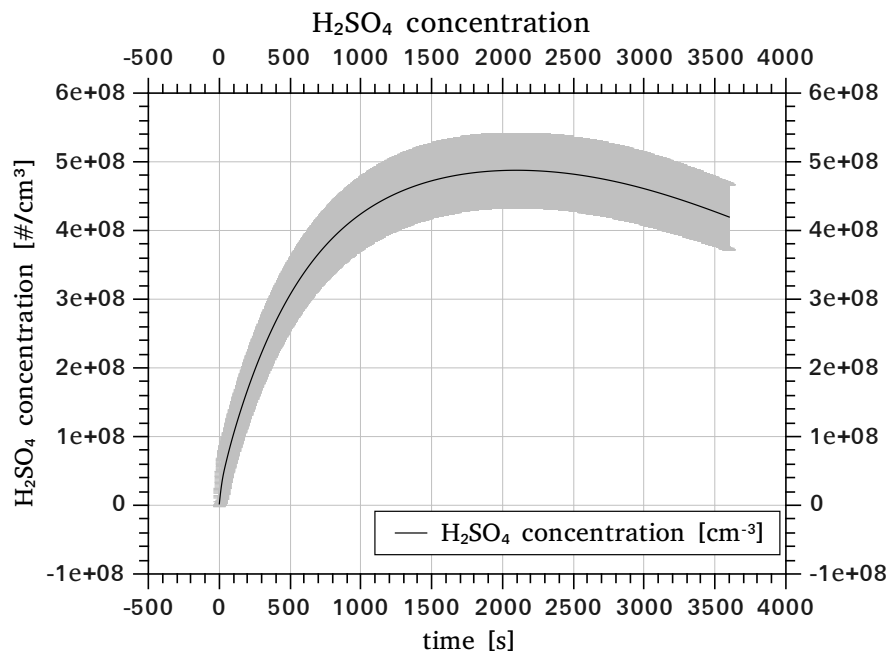
Printer-friendly Version

Interactive Discussion



Numerical  
simulations of the  
CLOUD chamber

J. Voigtländer et al.

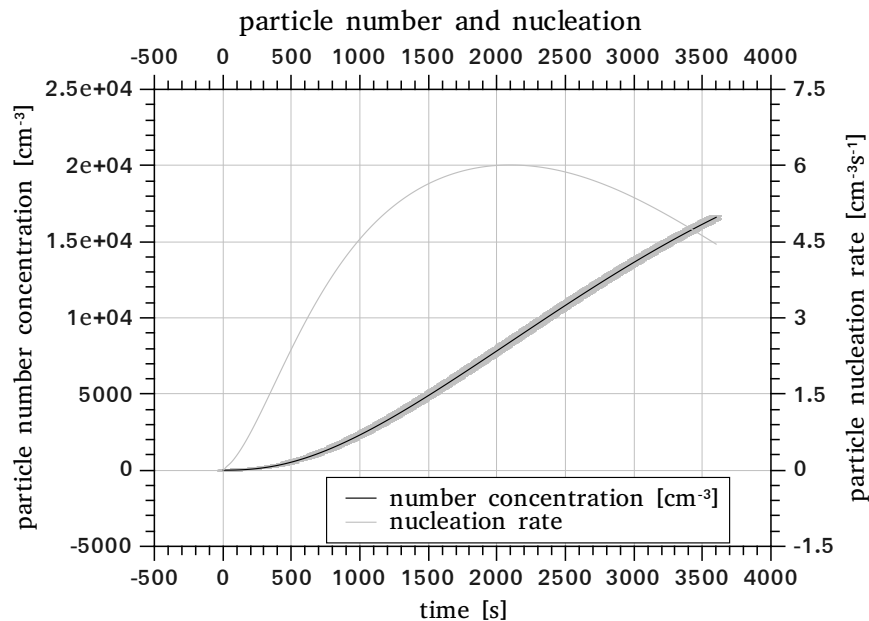


**Fig. 13.** Calculated  $\text{H}_2\text{SO}_4$  concentration assuming a constant production rate of  $1 \times 10^{-11} \text{ kg s}^{-1}$  and a 2-arc-shaped fan configuration.

[Title Page](#)[Abstract](#)[Introduction](#)[Conclusions](#)[References](#)[Tables](#)[Figures](#)[◀](#)[▶](#)[◀](#)[▶](#)[Back](#)[Close](#)[Full Screen / Esc](#)[Printer-friendly Version](#)[Interactive Discussion](#)

**Numerical  
simulations of the  
CLOUD chamber**

J. Voigtländer et al.

**Fig. 14.** Mean volume weighted nucleation rate.

Title Page

Abstract

Introduction

Conclusions

References

Tables

Figures

◀

▶

◀

▶

Back

Close

Full Screen / Esc

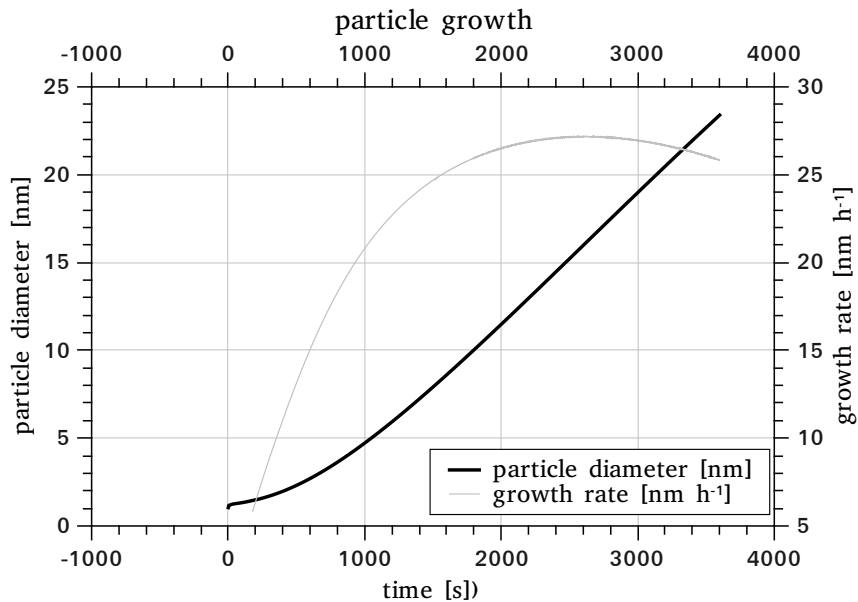
Printer-friendly Version

Interactive Discussion



**Numerical  
simulations of the  
CLOUD chamber**

J. Voigtländer et al.

**Fig. 15.** Mean volume weighted particle growth.[Title Page](#)[Abstract](#)[Introduction](#)[Conclusions](#)[References](#)[Tables](#)[Figures](#)[◀](#)[▶](#)[◀](#)[▶](#)[Back](#)[Close](#)[Full Screen / Esc](#)[Printer-friendly Version](#)[Interactive Discussion](#)